Theory of Excitation Energy Transfer in the Intermediate Coupling Case of Clusters

A. Kimura and T. Kakitani*

Department of Physics, Graduate School of Science, Nagoya University, Furo-cho, Chikusa-ku, Nagoya 464-8602, Japan

Received: December 10, 2002; In Final Form: October 3, 2003

Previously we presented a unified theory of excitation energy transfer (EET) in dimers, which is applicable to the intermediate coupling case by self-consistently solving the stochastic Liouville equation (Kimura, A.; Kakitani, T.; Yamato, T. *J. Phys. Chem. B* **2000** *104*, 9276). However, up to the present time, proper EET theory, which is applicable to the intermediate coupling case of clusters, was not established. In this paper, we contribute to such an intermediate coupling theory in cluster systems. We utilize the method of generalized master equations (GME). In the first step, we construct the memory function by the second-order perturbation theory of the excitonic interaction from a general point of view. Eventually, it is expressed by a Fourier transform of the overlap of the time-dependent fluorescence and the absorption spectra of the constituent molecules. We show that our new theory reduces to the Kenkre−Knox theory in the limit of fast vibrational relaxation and reduces to the Sumi theory of the hot transfer mechanism in the limit of fast decay of the memory function. In the next step, we introduce a renormalization function into this memory function. This renormalization includes a correction due to the contribution of powers of combination of the fourth- and the second-order correlation functions. By numerical calculations, we illustrate how the renormalization effect becomes significant as the excitonic coupling strength U becomes large. We applied this GME method to the EET between BChla molecules in B850 of the photosynthetic antenna system LH2. We found that the memory function calculated using the experimentally obtained optical spectra initially decays very rapidly (with time constant of about 5 fs) and has a plateau in the time region 10−25 fs. Because of this specific memory function, the calculated coherence length in the steady state was about 3. This GME method should be useful for the analysis of the mechanism of EET in many kinds of biological systems.

1. Introduction

It is an important problem to understand how solar energy is efficiently converted into chemical energy in photosynthesis. The excitation energy transfer (EET) in antenna systems takes place with remarkably high efficiency. To understand its mechanism, much study has been made for many types of photosynthetic antenna systems theoretically and experimentally.[1,2] Among them, crystal structures of the light harvesting system II (LH2) of *Rhodopseudomonas acidophila*[3] and *Rhodospirillum molischianum*[4] were elucidated in 1995 and 1996, respectively. These two systems are circular aggregates of bacteriochlorophyll a (BChla) molecules with high symmetry. Hence, many experimentalists and theorists are stimulated to elucidate the mechanism of EET in this system.[5−11] More recently, crystal structures of the photosystem I and II (PS I and II) from the thermophilic cyanobacterium *Synechococcus elongatus* were clarified.[12,13] Antenna systems involved in PS I and PS II are in close contact with the reaction centers and do not have significant symmetry in the chlorophylls aggregates. Together with the other antenna complexes, we find that the distances between pigments in the photosynthetic antenna systems distribute mostly over 10−20 Å and then the excitonic coupling strength U varies considerably from pair to pair. These results indicate that the origin of efficient EET in biological systems would not necessarily rely on the high symmetrical arrangement of the constituent molecules. Indeed, recently it was suggested that the EET from B800 to B850 in LH2 does not use the totally delocalized exciton state as a final state, but it uses the locally excited states of BChla molecules of B850 nearby the locally excited BChla molecules of B800.[14] This conclusion was obtained from the analysis of the experimentally obtained energy gap dependence of the rate of EET from the reconstructed B800 to B850.[15]

The mechanism of the EET changes depending on the excitonic coupling strength U and the coherence-destructive strength γ due to the electron−phonon interaction.[16] When U is much smaller than γ (weak coupling case), EET takes place by the Förster mechanism by means of the hopping from the localized excited state in the donor molecule to the acceptor. Förster derived the formula of this EET rate[17] and lead to Pauli's master equation (PME) in cluster. This corresponds to the case of the EET after completing vibrational relaxation in the donor and losing the coherent memory during EET. The rate formula is proportional to the overlap integral between the luminescence spectrum of the donor and the absorption spectrum of the acceptor.

On the other hand, when U is much larger than γ (strong coupling case), the excited state is little perturbed by the electron−phonon interaction and it is delocalized between donor and acceptor. This state is called exciton state, and the EET is called the exciton mechanism.[18]

When U is comparable with γ (intermediate coupling case), the excited state is considerably perturbed by the electron−phonon interaction. A completely delocalized exciton state between the donor and the acceptor is not formed, but only some

* Author to whom correspondence should be addressed. Tel. and fax: +81-52-789-3528. E-mail: kakitani@allegro.phys.nagoya-u.ac.jp.

10.1021/jp027667n CCC: $25.00
Published on Web 12/02/2003

part of the coherency is preserved during the EET between the donor and the acceptor.[19]

Some theoretical studies were made[20,21] to treat the EET in the cluster under the perturbation of the exciton−phonon interaction essentially based on the Redfield theory[22] where electron−phonon interaction is assumed to be small and is treated by the perturbation method. These approaches are only one step toward the intermediate coupling case starting from the strong coupling case. These approaches were useful to investigate how fast the exciton coherence domain, which is produced by the optical absorption, is shrunk with time after absorbing a photon.[20,21]

There were some studies to approach the EET in the intermediate coupling case using locally excited states as a base.[19,23−26] To describe the EET with coherent character at a very short time, Kenkre and Knox used a generalized master equation (GME) instead of PME and calculated the memory function by the second-order perturbation about the coupling strength U.[27,28] As a result, they succeeded in relating the memory function to the dynamical overlap of the optical spectra of the donor and acceptor molecules. On the other hand, Sumi extended the Förster's theory in order to give the rate of EET by the hot transfer mechanism in which the incoherent EET takes place on the way of vibrational relaxation in the donor excited state.[29] The rate formula is proportional to the overlap integral between the time-resolved fluorescence spectrum of the donor molecule[30] and the absorption spectrum of the acceptor molecule in the stationary state.

Recently, we developed a more complete theory of EET for dimers, which is applicable to the intermediate coupling case. This theory is formally applicable to all the values of the coupling strength U in the presence of homogeneous and inhomogeneous broadening.[19,23] In constructing the theory, the stochastic Liouville equation was solved self-consistently by adopting a decoupling procedure which corresponds to the factorization by a two-time correlation function of the excitation energy transfer interaction. Namely, the integro-differential equation of a renormalized propagator was solved. It was assumed that the two-time correlation function of the excitonic interaction decreases exponentially with time. By these assumptions, we could handle the theory nonperturbatively and analytically. As a result of it, we obtained some analytical formulas for the criteria among strong, intermediate, and weak coupling cases, which are functions of the coupling strength U, coherence-destructive strength γ, and the vibrational relaxation time in the excited state of donor.[19] However, the validity of the above two assumptions remains to be examined.

Under these circumstances, in this paper, we extend the above theory for the dimer system to cluster systems so that we can treat the EET in the antenna systems of photosynthesis. We do this by use of the GME method. The theory is made so that the initial state, just after photoabsorption, is in the nonequilibrium state by applying the three-state model in our dimer theory.[19,23] As a first step of such study, we treat the memory function by the second-order perturbation with respect to the coupling strength U. We derive a formula of the memory function of the GME, which is expressed by using optical spectra of pigments. This memory function can be reduced to the memory function of the Kenkre−Knox theory[27] when the donor state is put into the thermalization condition. On the other hand, when we force the Markovian condition to the memory function in our theory, we can derive Sumi's rate formula for a hot transfer mechanism.[29] Namely, we can show that our theory accommodates the Kenkre−Knox and Sumi theories as two extreme cases. In the second step, we improve the memory function in the GME by renormalizing the second-order memory function.

Constitution of this paper is as follows: In section 2, we derive the GME for the probability of the ith molecule being excited in the cluster after the pulse excitation at $t = 0$. In section 3, we demonstrate that the memory function can be expressed by the time-resolved emission spectrum and the absorption spectrum of each molecule in the cluster under the most general theoretical scheme. In section 4, we discuss the relationship between the present theory to the previous other theories. We also give theoretical foundation to the exponential form of the correlation function assumed in our dimer theory.[19] Section 5 is devoted to derive the renormalization function to the second-order memory function by which the effect of the powers of the second- and fourth-order correlation functions are incorporated. In section 6, numerical calculations are made in order to see how much the renormalization effect is important in the intermediate coupling case. Detailed analysis of the EET in B850 is also made. Some discussions are made in section 7.

2. Model and Theoretical Foundation

2.1. Preparation of the Nonequilibrium Excited State. The excited state immediately after photoabsorption of the donor molecule is in the nonequilibrium vibrational state. Then, in the intermediate coupling case, the EET may happen from the nonequilibrium state in the donor molecule. Such a case was treated in ref 23 where we explored the three-state model and we called this type-II EET. In the case of the cluster system, however, the dynamics of the EET becomes more complicated. So, let us consider that the cluster which consists of n molecules absorbs a light pulse. In the photoabsorption, the transition from the ground state to the excited state takes place by a certain molecule in the cluster. As in the same way as type II-EET, we choose the whole of the cluster in the ground state plus a photon before absorption as the state $|d\rangle$ (d state), where the thermal equilibrium is attained. And, we define the ith state as the state that the ith molecule is excited, where i is a number of site ($i = 1, ..., n$). This model is illustrated in Figure 1. In this figure, initially ($t = 0$), the jth molecule is excited. We calculate the probability $P_i(t)$ that the excitation energy is located at the ith molecule at time t. We do not confine the initially excited jth molecule to a specific molecule but it can be any molecule in the cluster.

Under the Condon approximation, we write the time-dependent Hamiltonian as follows

$$\mathscr{H}(t) = H + V_1(t) \tag{1}$$

$$H = H_0 + V_0 \tag{2}$$

$$H_0 = \sum_i H_i|i\rangle\langle i| + (H_p + E)|d\rangle\langle d| \tag{3}$$

$$V_0 = \sum_{ij} V_{ij}(|i\rangle\langle j| + |j\rangle\langle i|) \tag{4}$$

$$V_1(t) = \sum_j K_j(t)(|d\rangle\langle j| + |j\rangle\langle d|) \tag{5}$$

where H_i is the phonon Hamiltonian in the ith states, V_0 is the excitation transfer operator, H_p is the phonon Hamiltonian in the d state, E is the energy of an incident photon, and $V_1(t)$ is the excitation operator which excites the molecular system by light pulse. In this Hamiltonian, we assume that the operator $H_i - H_p$ for $i = 1, ..., n$ is commutable with each other. This implies that the vibrational modes of phonons at each state are

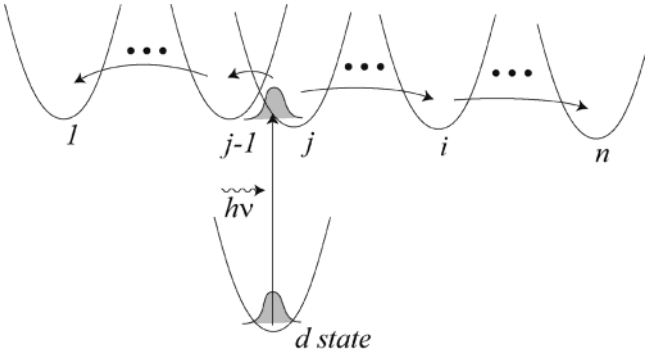

Figure 1. The model of the EET in the cluster system. The *d* state is the ground state of the whole of cluster plus a photon before absorbed. We consider *n* kinds of excited states where only one species of molecule, namely, the *i*th molecule, is excited ($i = 1, ..., n$). In the figure, initially the *j*th molecule is excited. After it, the EET takes place to all the sites of cluster.

independent of each other because the molecules in the cluster are separated well from each other. And, we assume that the strength of the interaction $|K_j(t)|$ between a photon and each molecule is sufficiently weak. Then, we adopt the perturbation method with respect to $K_j(t)$ for our theory. We assume the density operator at $t = 0$ as

$$\rho(0) \equiv |d\rangle\rho_d\langle d| \tag{6}$$

where $\rho_d = e^{-\beta(H_p+E)}/\mathrm{Tr}[e^{-\beta(H_p+E)}]$. Tr represents the trace over the vibrational state. It is equivalent to the density operator $\rho_p = e^{-\beta H_p}/\mathrm{Tr}[e^{-\beta H_p}]$ of the phonon field. Then, the density operator is written as follows

$$\rho(t) = \exp_+\left\{-\frac{i}{\hbar}\int_0^t \mathscr{H}(t')\,dt'\right\}|d\rangle\rho_p\langle d|\,\exp_-\left\{\frac{i}{\hbar}\int_0^t \mathscr{H}(t')\,dt'\right\} \tag{7}$$

Hence, the probability at the *i*th state as a function of *t* is given by

$$P_i(t) = \mathrm{Tr}[\langle i|\rho(t)|i\rangle] \tag{8}$$

As shown in Appendix A, $P_i(t)$ can be rewritten as

$$P_i(t) \equiv \sum_j P_j(0)\mathrm{Tr}[\langle j|\rho_E|j\rangle\langle j|e^{iHt/\hbar}|i\rangle\langle i|e^{-iHt/\hbar}|j\rangle] \tag{9}$$

where $P_j(0)$ (for $j = 1, ..., n$) represents the probability that the *j*th molecule is excited at $t = 0$. And, ρ_E is the following density operator

$$\rho_E = \sum_j \frac{1}{2\pi\hbar}\int_{-\infty}^{\infty} d\sigma \frac{e^{-iE\sigma/\hbar}}{I_j(E)}\, e^{iH_j\sigma/2\hbar}e^{-iH_p\sigma/\hbar}\rho_p e^{iH_j\sigma/2\hbar}|j\rangle\langle j| \tag{10}$$

where $I_j(E)$ is the absorption spectrum of the *j*th site which is normalized as $\int dE I_j(E) = 1$. The variable σ represents the time since photoabsorption. The density operator ρ_E represents the nonequilibrium distribution of the phonon at each site of molecules immediately after a light pulse excitation. This derivation followed the work of Sumi.[29]

2.2. Generalized Master Equation. We derive some formula of the GME for the probability $P_i(t)$. We do it because theoretical techniques used in the derivation are inevitable for the further study in this paper. We introduce the projection operator (projector), which is able to derive the memory function depending on the initial nonequilibrium state.

$$\langle i|\mathscr{P}A|j\rangle = \langle i|(1-\mathscr{Q})A|j\rangle = \delta_{ij}\langle i|\rho_E|i\rangle\mathrm{Tr}[\langle i|A|i\rangle] \tag{11}$$

where $\mathscr{P}^2 = \mathscr{P}$ holds. Apparently, the projector $\mathscr{P}$ of eq 11 is capable of erasing the off-diagonal elements in the electronic excited state of the operator A averaging it over the phonon state and makes the memory function keep the memory at the initial nonequilibrium state. To derive the GME by the projector $\mathscr{P}$, we define the Liouville operator as $L = L_0 + L_1$, $L_0A = [H_0, A]$, and $L_1B = [V_0, B]$ and redefine the density superoperator as $\rho_j(t) = \exp(-iLt/\hbar)|jj\rangle\langle jj|\rho_E\rangle$, where $|ij\rangle$ represents the ket vector of the electronic states in the Liouville space. Thus, the Liouville equation by the interaction representation can be written as follows

$$i\hbar\frac{d\rho_{Ij}(t)}{dt} = [V_I(t),\rho_{Ij}(t)] = L_1(t)\rho_{Ij}(t) \tag{12}$$

where $\rho_{Ij}(t) = e^{iL_0t/\hbar}\rho_j(t)$ and $V_I(t) = e^{iH_0t/\hbar}V_0e^{-iH_0t/\hbar}$. Hence using the Liouville space representation, we can rewrite the probability $P_i(t)$ as follows

$$P_i(t) = \sum_j P_j(0)\mathrm{Tr}[\langle ii|\rho_{Ij}(t)\rangle] \tag{13}$$

In the Appendix B, we have derived some formulas of the GME by the more general scheme than before.

Because $\mathscr{Q}L_1(t)\mathscr{P} = 0$ holds, taking the trace over the phonon states of the GME of eq B11, we can obtain the following equation

$$\frac{d\mathrm{Tr}[\langle ii|\rho_{Ij}(t)\rangle]}{dt} = \sum_k \int_0^t dt_1 M_{ik}(t, t_1)\mathrm{Tr}[\langle kk|\rho_{Ij}(t_1)\rangle] \tag{14}$$

where we assumed $\mathscr{Q}\rho_{Ij}(0) = 0$ for all *j*. In this result, the memory function can be written as

$$M_{ij}(t,t_1) \equiv -\frac{1}{\hbar^2}\mathrm{Tr}\left[\langle ii|L_1(t)\exp_+\left[-\frac{i}{\hbar}\int_{t_1}^t dt_2\mathscr{Q}L_1(t_2)\right]L_1(t_1)|jj\rangle\langle jj|\rho_E\rangle\right] \tag{15}$$

Multiplying $\mathrm{Tr}(\langle ii|\rho_{Ij}(t)\rangle)$ by $P_j(0)$ in eq 14 and summing it up over the electronic excited states *j* of all molecular sites, we obtain the generalized master equation as follows

$$\frac{dP_i(t)}{dt} = \sum_{k\neq i}\int_0^t dt_1[M_{ik}(t,t_1)P_k(t_1) - M_{ki}(t,t_1)P_i(t_1)] \tag{16}$$

where we used the sum rule $\sum_i M_{ij}(t,t_1) = 0$. Evidently, the memory function $M_{ij}(t,t_1)$ of eq 15 naturally includes the memory of the initial nonequilibrium state. Consequently, owing to eq 15, we can calculate the dynamics of the EET in the cluster system during vibrational relaxation.

3. Second-Order Memory Function

To investigate the mechanism of the EET by the GME, we need to evaluate the memory function of eq 15. In a rather weak coupling case, we can approximate it by the second-order perturbation with respect to $L_1(t)$ as follows

$$M_{ij}(t,t_1) \equiv -\frac{1}{\hbar^2}\langle L_1(t)L_1(t_1)\rangle_{E,ij} \tag{17}$$

where $\langle\cdots\rangle_{E,ij} \equiv \mathrm{Tr}[\langle ii|\cdots|jj\rangle\langle jj|\rho_E\rangle]$. We call it the second-order memory function hereafter.

In this section, we show that we can connect this memory function with the optical spectra of respective molecules in the cluster system. In the Hilbert space, the memory function of eq 17 in the case of $i \neq j$ can be rewritten as follows

$$M_{ij}(t,t_1) = 2\mathrm{Re}[\langle\langle j|V_I(t)|i\rangle\langle i|V_I(t_1)|j\rangle\rangle_{E,j}]/\hbar^2 \qquad (18)$$

where $\langle\cdots\rangle_{E,j} \equiv \mathrm{Tr}[\langle j|\rho_E|j\rangle\cdots]$.

Since $H_i - H_p$ is commutable with $H_j - H_p$ ($i \neq j$) in our treatment, the correlation function can be rewritten as follows

$$\langle\langle j|V_I(t)|i\rangle\langle i|V_I(t_1)|j\rangle\rangle_{E,j} = V_{ij}^2\langle e^{iH_j t/\hbar}e^{-iH_p(t-t_1)/\hbar}e^{-iH_j t_1/\hbar}\rangle_{E,j}\langle e^{iH_p(t-t_1)/\hbar}e^{-iH_i(t-t_1)/\hbar}\rangle_p \qquad (19)$$

where $\langle\cdots\rangle_p$ represents the average over canonical ensemble $\mathrm{Tr}[\rho_p\cdots]$ for vibrations in the phonon field. Let us define the time difference as $\mu \equiv t - t_1$ and the time average as $\tau \equiv (t + t_1)/2$. Applying Fourier transformation with μ to eq 19, we obtain the following convolution

$$\int_{-\infty}^{\infty} d\mu e^{-iE'\mu/\hbar}\langle\langle j|V_I(\tau+\mu/2)|i\rangle\langle i|V_I(\tau-\mu/2)|j\rangle\rangle_{E,j} = \frac{1}{2\pi\hbar}\int_{-\infty}^{\infty} dE''\int_{-\infty}^{\infty} d\mu \langle e^{iH_j(\tau+\mu/2)/\hbar}e^{-i(H_p+E'')\mu/\hbar}e^{-iH_j(\tau-\mu/2)/\hbar}\rangle_{E,j} \times \int_{-\infty}^{\infty} d\xi\langle e^{-i(E'-E'')\xi/\hbar}e^{iH_p\xi/\hbar}e^{-iH_i\xi/\hbar}\rangle_p \qquad (20)$$

In this equation, the ξ integration of the right-hand side of eq 20 is equivalent to the absorption spectrum of $I_j(E)$ at the jth molecule

$$I_j(E) = \frac{1}{2\pi\hbar}\int_{-\infty}^{\infty} d\sigma e^{-iE\sigma/\hbar}\langle e^{iH_j\sigma/\hbar}e^{-iH_p\sigma/\hbar}\rangle_p \qquad (21)$$

where it satisfies the normalization $\int dE I_j(E) = 1$. As shown in Appendix C, we found that the μ integration of the right-hand side of eq 20 is proportional to the time-resolved flourescence spectrum for the light pulse excitation.[30] Namely, we obtain the following fluorescence spectrum

$$L_j(E,E'',\tau) = \frac{1}{2\pi\hbar}\int_{-\infty}^{\infty} d\mu\langle e^{iH_j(\tau+\mu/2)/\hbar}e^{-i(H_p+E'')\mu/\hbar}e^{-iH_j(\tau-\mu/2)/\hbar}\rangle_{E,j} \qquad (22)$$

where E and E'' are the energies of the incident and the emission of photon, respectively, and the spectrum satisfies the normalization as $\int L_j(E,E'',\tau)\, dE'' = 1$. It should be noticed that this fluorescence spectrum is a function of time since it changes through the vibrational relaxation in the excited state. Consequently, applying inverse Fourier transformation to eq 20, we obtain the final form of the correlation function as follows

$$\langle\langle j|V_I(t)|i\rangle\langle i|V_I(t_1)|j\rangle\rangle_{E,j} = V_{ij}^2\int_{-\infty}^{\infty} d(\Delta E)e^{i\Delta E(t-t_1)/\hbar}F_{ij}(E,\Delta E,(t+t_1)/2) \qquad (23)$$

where $F_{ij}(E,\Delta E,\tau)$ is the overlap integral of the time-dependent fluorescence spectrum and the absorption spectrum shifted by ΔE as follows

$$F_{ij}(E,\Delta E,\tau) = \int_{-\infty}^{\infty} dE' L_j(E,E',\tau)I_i(E'-\Delta E) \qquad (24)$$

Hence, the memory function can be written as follows

$$M_{ij}(t,t_1) = \frac{2V_{ij}^2}{\hbar^2}\int_{-\infty}^{\infty} d(\Delta E)\cos(\Delta E(t-t_1)/\hbar)\times \int_{-\infty}^{\infty} dE' L_j(E,E',(t+t_1)/2)I_i(E'-\Delta E) \qquad (25)$$

where ΔE implies the quantum mechanical fluctuation in the EET. Namely, the breakdown of the energy conservation for EET is allowed by the amount of ΔE.

So far we have implicitly considered the homogeneous system. However, it is usual that the system is inhomogeneous in molecular aggregates. Namely, the absorption peak or the fluorescence peak is broadened. In the following, we show that even if such inhomogeneity exists, the resultant formula of eq 25 does not change if we reread the fluorescence spectrum $L_j(E,E',(t+t_1)/2)$ and the absorption spectrum as ones which include such inhomogeneous effect. Let us denote the amplitude of the fluctuation of energy at site i as Δ_i. Then, the H_0 in eq 3 should be rewritten as

$$H_0 = \sum_i (H_i + \Delta_i)|i\rangle\langle i| + (H_p + E)|d\rangle\langle d| \qquad (26)$$

Since Δ_i is not an operator, we can formally include it into H_i. That is, we redefine $H_i + \Delta_i$ as H_i. Let the normalized distribution function of Δ_i be $f_i(\Delta_i)$. Then the average over this distribution is made for all the quantities in this paper. Applying such average to $M_{ij}(t,t_1)$ in eq 25, we can write

$$\bar{M}_{ij}(t,t_1) = \frac{2V_{ij}^2}{\hbar^2}\int_{-\infty}^{\infty} d(\Delta E)\cos(\Delta E(t-t_1)/\hbar)\times \int_{-\infty}^{\infty} dE'\bar{L}_j(E,E',(t+t_1)/2)\bar{I}_i(E'-\Delta E) \qquad (27)$$

where

$$\bar{L}_j(E,E',(t+t_1)/2) = \int_{-\infty}^{\infty} f_j(\Delta_j)d\Delta_j L_j(E,E',(t+t_1)/2) \qquad (28)$$

$$\bar{I}_i(E'-\Delta E) = \int_{-\infty}^{\infty} f_i(\Delta_i)\, d\Delta_i I_i(E'-\Delta E) \qquad (29)$$

Indeed, $\bar{L}_j$ and $\bar{I}_i$ are the time-dependent fluorescence spectrum and absorption spectrum, which are experimentally observed in the inhomogeneous systems. So far as we use the experimental data for the optical spectra, eq 25 will always hold true by replacing L_j and I_i with $\bar{L}_j$ and $\bar{I}_i$, respectively.

4. Relation to the Other Theories

4.1. Relation to the Kenkre−Knox Theory and the Sumi Formula. Let us consider the case when the time of vibrational relaxation in the donor molecule is much shorter than that of the EET. In this case, we approximate the initial state to the thermal equilibrium after completing vibrational relaxation at the donor molecule. Hence, we rewrite the average $\langle\cdots\rangle_{E,j}$ in eq 22 as $\langle\cdots\rangle_j \equiv \mathrm{Tr}[\rho_j\cdots]$, where $\rho_j \equiv e^{-\beta H_j}/\mathrm{Tr}[e^{-\beta H_j}]$. Then, it gives us the following result

$$M_{ij}^{\mathrm{Th}}(t,t_1) = \frac{2V_{ij}^2}{\hbar}\int_{-\infty}^{\infty} d(\Delta E/\hbar)\cos(\Delta E(t-t_1)/\hbar)\times \int_{-\infty}^{\infty} dE' L_j(E')I_i(E'-\Delta E) \qquad (30)$$

where we defined the fluorescence spectrum of the jth molecule as $L_j(E')$. This result is equivalent to the memory function of GME in the Kenkre−Knox theory.[27]

Next, let us consider the case that the EET takes place during vibrational relaxation when the initial excited state is produced by the pulse light absorption. Furthermore, we assume that the coherent memory is completely lost always. In this case, we can apply Markovian approximation to the memory function as

$$M_{ij}^{\mathrm{Ma}}(\tau+\mu/2,\tau-\mu/2)=\delta(\mu)\int_{-\infty}^{\infty}\mathrm{d}\mu' M_{ij}(\tau+\mu'/2,\tau-\mu'/2) \tag{31}$$

Integrating eq 31 with time μ, we obtain the rate of the EET from the jth to the ith molecules as follows

$$k_{ij}(E,t)=\frac{2\pi V_{ij}^2}{\hbar}\int_{-\infty}^{\infty}\mathrm{d}E' L_j(E,E',t)I_i(E')\equiv\frac{2\pi V_{ij}^2}{\hbar}(\mathrm{FC})_{ij,E,t} \tag{32}$$

In this case, the GME reduces to the following equation

$$\frac{\mathrm{d}P_i(t)}{\mathrm{d}t}=\sum_{j\neq i}\{k_{ij}(E,t)P_j(t)-k_{ji}(E,t)P_i(t)\} \tag{33}$$

In the above, $(\mathrm{FC})_{ij,E,t}$, which may be called the transient Franck−Condon factor, is equal to $F_{ij}(E,0,t)$ in eq 24. This result is equivalent to the Sumi's rate formula of the EET by the hot transfer mechanism by light pulse excitation.[29] In the case that the t dependence of $k_{ij}(E,t)$ in eq 33 can be neglected, the PME is obtained.

Namely, we found that the memory function of eq 25, which is expressed by the theory of the second-order perturbation with respect to the excitonic coupling strength, has the ability to cover the vibrationally relaxing EET in the intermediate coupling case.

In Figure 2, we show schematically the relationship of the spectral overlap used in (a) the Förster theory, (b) the Sumi theory, (c) the Kenkre−Knox theory, and (d) the present theory.

4.2. Relation to Our Dimer Theory. In our dimer theory,[19] we assumed that the correlation function $\langle\langle m|V_I(t)V_I(t_1)|m\rangle\rangle_d$ decreases exponentially with time, where $|m\rangle$ is the excited state of donor after photoabsorption and $|a\rangle$ is the excited state of acceptor after excitation enegy transferred. Namely, we assumed that the correlation function can be expressed as

$$\langle\langle m|V_I(t)V_I(t_1)|m\rangle\rangle_d=U^2\exp(-(t-t_1)/\tau_c(t_1)) \tag{34}$$

where the correlation time can be expressed as $\tau_c(t_1)=\pi\hbar(\mathrm{FC})_{t_1}$ and the excitonic coupling strength between the donor and acceptor was expressed as U. We derive the necessary condition that correlation function eq 34 is obtained, based on the present theory.

Let us consider that the time-resolved fluorescence spectrum of the donor molecule and the absorption spectrum of the acceptor molecule are written by the following Lorentzian

$$L_m(E,E',\tau)=\frac{1}{\pi}\frac{\Gamma_m(E,\tau)}{(E'-E_m)^2+\Gamma_m^2(E,\tau)} \tag{35}$$

$$I_a(E')=\frac{1}{\pi}\frac{\Gamma_a}{(E'-E_a)^2+\Gamma_a^2} \tag{36}$$

where $\Gamma_m(E,\tau)$ and E_m are the homogeneous line width (half width at half-maximum) and the peak position in the spectrum of the donor molecule. We assumed that $\Gamma_m(E,\tau)$ depends on the energy E of incident photon and the time τ at the observation. Similarly, Γ_a and E_a are the parameters of the acceptor molecule. These spectra satisfy the normalization conditions in the above section. Substituting these spectra into eq 23, we obtain the following result

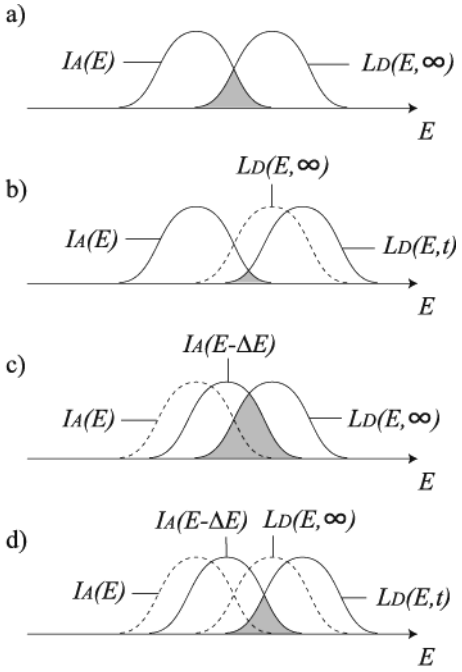

Figure 2. Four kinds of overlap integral of the absorption spectrum and the fluorescence spectrum. (a) Overlap integral used in the Förster mechanism $I_A(E)$ is the absorption spectrum of acceptor. $L_D(E,\infty)$ is the fluorescence spectrum obtained from the equilibrium state of the donor excited state. (b) Overlap integral used in the hot transfer mechanism of Sumi theory. $L_D(E,t)$ is the fluorescence spectrum obtained from the donor excited state on the way of the vibrational relaxation. (c) Overlap integral used in the memory function of the Kenkre−Knox theory. $I_A(E-\Delta E)$ is the absorption spectrum of acceptor shifted by $-\Delta E$ in order to incorporate the coherent interaction effect. (d) Overlap integral used in the present theory. Both of the fluorescence spectrum from the donor excited state on the way of vibrational relaxation $L_D(E,t)$ and the absorption spectrum of acceptor incorporating the coherent interaction effect $I_A(E-\Delta E)$ are taken into account.

$$M_{am}(\tau+\mu/2,\tau-\mu/2)=\frac{2U^2}{\hbar^2}\cos(\Delta G_{am}\mu/\hbar)\exp[-(\Gamma_m(E,\tau)+\Gamma_a)\mu/\hbar] \tag{37}$$

with $\Delta G_{am}=E_m-E_a$.

On the other hand, substituting eqs 35 and 36 into eq 32, we can represent the transient Franck−Condon factor between $|a\rangle$ and $|m\rangle$ states as follows

$$(\mathrm{FC})_{am,E,\tau}=\frac{\Gamma_m(E,\tau)+\Gamma_a}{\pi[(\Gamma_m(E,\tau)+\Gamma_a)^2+\Delta G_{am}^2]} \tag{38}$$

Resolving $\Gamma_m(E,\tau)+\Gamma_a$ from eq 38 and substituting it into the eq 37, we represent the memory function as follows

$$M_{am}(\tau+\mu/2,\tau-\mu/2)=\frac{2U^2}{\hbar^2}\cos(\Delta G_{am}\mu/\hbar)\exp\left[-\frac{1+(1-4\pi(\mathrm{FC})_{am,E,\tau}\Delta G_{am}^2)^{1/2}}{2\pi\hbar(\mathrm{FC})_{am,E,\tau}}\mu\right] \tag{39}$$

In the case $\Delta G_{am} \simeq 0$, we can approximate the above function as

$$M_{am}(\tau + \mu/2,\tau - \mu/2) = \frac{2U^2}{\hbar^2} \exp\left[-\frac{\mu}{\pi\hbar(\mathrm{FC})_{am,E,\tau}}\right] \quad (40)$$

Combining eqs 34 and 18, we can reproduce eq 40. Then, we find that the form of the correlation function in eq 34 is suitable in the case that the spectra of the molecules are expressed by the Lorenzian and satisfy the condition $E_m \simeq E_a$. Namely, they are the necessary condition for expressing the correlation function by an exponential form. We can relax this condition to some extent by the treatment of cummulant expansion of correlation function based on the Kubo theory.[31] This theoretical calculation is given elsewhere.[32] Under such treatment, the coherence-destructive strength γ is defined as

$$\gamma_{am} = \frac{1}{\pi(\mathrm{FC})_{am,E,\tau}} \quad (41)$$

in accordance with eq 67 in ref 19.

5. Renormalization of the Second-Order Memory Function

When the coupling strength becomes large, the role of the higher-order term of $L_1(t)$ in the memory function of eq 15 becomes significant. Then, we conduct renormalization of the memory function by including the higher order terms. Namely, we expect that the memory function is expressed as follows

$$M_{ij}(t,t_1) = -\frac{1}{\hbar^2}\langle L_1(t)L_1(t_1)\rangle_{E,ij} R_{ij}(E,t,t_1) \quad (42)$$

where $R_{ij}(E,t,t_1)$ represents the renormalization function.

Comparing eq 42 with eq 15, we can represent $R_{ij}(E,t,t_1)$ as follows

$$R_{ij}(E,t,t_1) \equiv \frac{\langle L_1(t)U(t,t_1)L_1(t_1)\rangle_{E,ij}}{\langle L_1(t)L_1(t_1)\rangle_{E,ij}} \quad (43)$$

where the propagator $U(t,t_1)$ is written as

$$U(t,t_1) \equiv \exp_+\left[-\frac{i}{\hbar}\int_{t_1}^{t} dt'_2 \mathcal{Q}L_1(t'_2)\right] \quad (44)$$

In eq 43, we should be careful of the fact that the second-order memory function $\langle L_1(t)L_1(t_1)\rangle_{E,ij}$ should not be zero. When $\langle L_1(t)L_1(t_1)\rangle_{E,ij} = 0$ holds, we should put $M_{ij}(t,t_1) = 0$. In the following, using the projection operator method,[33] we derive the equation of $R_{ij}(E,t,t_1)$. From eq 44, $U(t,t_1)L_1(t_1)$ satisfies the following equation

$$\frac{\partial U(t,t_1)L_1(t_1)}{\partial t} = -\frac{i}{\hbar}\mathcal{Q}L_1(t)U(t,t_1)L_1(t_1) \quad (45)$$

We introduce the following time-dependent projection operator $X(t)$

$$X(t)\hat{A} = (1 - Y(t))\hat{A} = \frac{\langle L_1(t)\hat{A}\rangle_{E,ij}}{\langle L_1(t)L_1(t_1)\rangle_{E,ij}} L_1(t_1) \quad (46)$$

where we abbreviated the indices i, j, and time t_1 in the left-hand term for simplicity. Using the operator $X(t)$ and eq 45, we can derive a closed equation for $X(t,t_1)U(t,t_1)L_1(t_1)$. According to Appendix B, we obtain

$$\frac{\partial X(t)U(t,t_1)L_1(t_1)}{\partial t} = -\frac{i}{\hbar}X(t)\mathcal{Q}L_1(t)X(t)U(t,t_1)L_1(t_1) - \frac{1}{\hbar^2}\int_{t_1}^{t} dt_2 (X(t)\mathcal{Q}L_1(t) + i\hbar\dot{X}(t))\exp_+\left[-\frac{i}{\hbar}\int_{t_2}^{t} dt_3 (Y(t_3)\mathcal{Q}L_1(t_3) - i\hbar\dot{Y}(t_3))\right] Y(t_2)\mathcal{Q}L_1(t_2)X(t_2)U(t_2,t_1)L_1(t_1) \quad (47)$$

In the following, we make the approximation that the operator $\exp_+(\cdots)$ in eq 47 is put as 1. Multiplying $L_1(t)$ to eq 47 from the left-hand side and taking the average of it by $\langle\cdots\rangle_{E,ij}$, we obtain

$$\frac{\partial R_{ij}(E,t,t_1)}{\partial t} = -\frac{i}{\hbar}Z_{ij}^{(1)}(E,t,t_1)R_{ij}(E,t\hbar) - \frac{1}{\hbar^2}\int_{t_1}^{t} dt_2 (Z_{ij}^{(2)}(E,t,t_2,t_1) + Z_{ij}^{(3)}(E,t,t_2,t_1))R_{ij}(E,t_2,t_1) \quad (48)$$

where

$$Z_{ij}^{(1)}(E,t,t_1) \equiv \frac{\langle L_1(t)L_1(t)L_1(t_1)\rangle_{E,ij}}{\langle L_1(t)L_1(t_1)\rangle_{E,ij}} \quad (49)$$

$$Z_{ij}^{(2)}(E,t,t_2,t_1) \equiv i\hbar\langle L_1(t)L_1(t_1)\rangle_{E,ij}\frac{\partial}{\partial t}\frac{\langle L_1(t)L_1(t_2)L_1(t_1)\rangle_{E,ij}}{\langle L_1(t)L_1(t_1)\rangle_{E,ij}} \quad (50)$$

$$Z_{ij}^{(3)}(E,t,t_2,t_1) \equiv \frac{\langle L_1(t)L_1(t)\mathcal{Q}L_1(t_2)L_1(t_1)\rangle_{E,ij}}{\langle L_1(t)L_1(t_1)\rangle_{E,ij}} \quad (51)$$

We can express the three types of correlation functions $\langle L_1(t)L_1(t_1)\rangle_{E,ij}$, $\langle L_1(t)L_1(t_2)L_1(t_1)\rangle_{E,ij}$, and $\langle L_1(t)L_1(t)\mathcal{Q}L_1(t_2)L_1(t_1)\rangle_{E,ij}$ by the quantities involved in H_0 and V_0 of eqs 3 and 4. Its detailed expression using $V_I(t)$ will be published elsewhere.[34]

Basically we can solve eq 48 numerically. However, it is usually time-consuming for clusters. Then, we try to simplify the integro-differential equation for $R_{ij}(E,t_2,t_1)$ in eq 48. The correlation function $\langle L(t)L(t_2)L(t_1)\rangle_{E,ij}$ is rewritten by the Heisenberg expression as follows

$$\langle L(t)L(t_2)L(t_1)\rangle_{E,ij} = -2i\mathrm{Im}[\langle\langle j|V_I(t)|i\rangle\langle i|V_I(t_2)V_I(t_1)|j\rangle\rangle_{E,j} + \langle\langle j|V_I(t_2)|i\rangle\langle i|V_I(t)V_I(t_1)|j\rangle\rangle_{E,j} + \langle\langle j|V_I(t_1)|i\rangle\langle i|V_I(t)V_I(t_2)|j\rangle\rangle_{E,j}] \quad (52)$$

Similarly, the correlation function $\langle L_1(t)L_1(t)\mathcal{Q}L_1(t_2)L_1(t_1)\rangle_{E,ij}$ is rewritten as follows

$$\begin{aligned}\langle L_1(t)L_1(t)\mathcal{Q}L_1(t_2)L_1(t_1)\rangle_{E,ij} = {} & 2\mathrm{Re}[-\langle\langle j|V_I(t)V_I(t)|j\rangle\langle j|V_I(t_2)V_I(t_1)|j\rangle\rangle_{E,j} - \\ & \langle\langle j|V_I(t)V_I(t)|j\rangle\langle j|V_I(t_2)V_I(t_1)|j\rangle\rangle_{E,j} - \\ & \langle\langle j|V_I(t_2)V_I(t)|j\rangle\langle j|V_I(t)V_I(t_1)|j\rangle\rangle_{E,j} - \\ & \langle\langle j|V_I(t_1)V_I(t)|j\rangle\langle j|V_I(t)V_I(t_2)|j\rangle\rangle_{E,j}] + \\ & 4\mathrm{Re}[\langle\langle j|V_I(t)V_I(t)|j\rangle\rangle_{E,j}]\mathrm{Re}[\langle\langle j|V_I(t_2)V_I(t_1)|j\rangle\rangle_{E,j}]\end{aligned} \quad (53)$$

Using the relation $1 = \mathcal{P} + \mathcal{Q}$, we can rewrite the correlation functions as follows

$$\langle\langle j|V_I(t)|i\rangle\langle i|V_I(t_2)V_I(t_1)|j\rangle\rangle_{E,j} = \langle\langle j|V_I(t)|i\rangle\langle i|\mathcal{Q}V_I(t_2)V_I(t_1)|j\rangle\rangle_{E,j} \quad (54)$$

$$\langle\langle j|V_I(t_1)V_I(t'_1)|j\rangle\langle j|V_I(t_2)V_I(t'_2)|j\rangle\rangle_{E,j} = \langle\langle j|V_I(t_1)V_I(t'_1)|j\rangle\rangle_{E,j}\langle\langle j|V_I(t_2)V_I(t'_2)|j\rangle\rangle_{E,j} + \langle\langle j|V_I(t_1)V_I(t'_1)|j\rangle\langle j|\mathcal{Q}V_I(t_2)V_I(t'_2)|j\rangle\rangle_{E,j} \quad (55)$$

The right-hand side in eq 54 and the second term of rhs in eq 55 work through the virtual state at time t_2 because of the operator $\mathcal{Q}$. In the intermediate coupling case where the exciton−phonon interaction is considerably strong, we assume that the virtual quantum state at t_2 will play a small role in this correlation function. Then, we neglect all the terms which involve $\mathcal{Q}$ in the Heisenberg expression for eqs 52 and 53. Namely, we obtain

$$Z_{ij}^{(1)}(E,t,t_1) \simeq 0 \qquad Z_{ij}^{(2)}(E,t,t_1) \simeq 0 \quad (56)$$

$$\langle\langle j|V_I(t_1)V_I(t'_1)|j\rangle\langle j|V_I(t_2)V_I(t'_2)|j\rangle\rangle_{E,j} \simeq \langle\langle j|V_I(t_1)V_I(t'_1)|j\rangle\rangle_{E,j}\langle\langle j|V_I(t_2)V_I(t'_2)|j\rangle\rangle_{E,j} \quad (57)$$

and we assume the time reversal approximation

$$\langle\langle j|V_I(t)V_I(t')|j\rangle\rangle_{E,j} = \langle\langle j|V_I(t')V_I(t)|j\rangle\rangle_{E,j} \quad (58)$$

We also assume that $\langle\langle j|V_I(t)V_I(t')|j\rangle\rangle_{E,j}$ is real. In this case, we obtain a relation

$$\langle L_1(t)L_1(t_1)\rangle_{E,ij} = -2\mathrm{Re}[\langle\langle j|V_I(t)V_I(t_1)|j\rangle\rangle_{E,j}] \quad (59)$$

Substituting eqs 57 and 58 into eq 53 and using eq 59, we obtain

$$Z_{ij}^{(3)}(E,t,t_2,t_1) = 2\mathrm{Re}[\langle\langle j|V_I(t)V_I(t_2)|j\rangle\rangle_{E,j}] \quad (60)$$

Substituting eqs 56 and 60 into eq 48, we finally obtain

$$\frac{\partial R_{ij}(E,t,t_1)}{\partial t} = -\frac{2}{\hbar^2}\int_{t_1}^{t} \mathrm{d}t_2 \mathrm{Re}[\langle\langle j|V_I(t)V_I(t_2)|j\rangle\rangle_{E,j}]R_{ij}(E,t_2,t_1) \quad (61)$$

The kernel in the integral of this equation has the same form as the second-order memory function in eq 18. Therefore, we can evaluate it in the same way as the method in section 3 with use of the time-resolved fluorescence and the absorption spectra. Substituting its $R_{ij}(E,t,t_1)$ into eq 42, we obtain the renormalized memory function.

We can solve eq 61 analytically in a special case that the two-time correlation function is expressed by an exponential form as follows

$$\langle\langle j|V_I(t)V_I(t')|j\rangle\rangle_{E,j} = V_{ij}^2 \exp(-\gamma|t-t'|/\hbar) \quad (62)$$

In this case, we obtain the following integro-differential equation for $R_{ij}(t_2, t_1)$

$$\frac{\partial R_{ij}(t,t_1)}{\partial t} = -\frac{2V_{ij}^2}{\hbar^2}\int_{t_1}^{t}\mathrm{d}t_2 \exp(-(t-t_2)/\tau)R_{ij}(t_2,t_1) \quad (63)$$

Putting the initial conditions

$$R_{ij}(t_1,t_1) = 1 \qquad \frac{\partial R_{ij}(t_1,t_1)}{\partial t} = 0 \quad (64)$$

we obtain the solution

$$R_{ij}(t,t_1) = \mathrm{e}^{-\gamma(t-t_1)/\hbar}\left[\cosh\left(\frac{\gamma(\xi_{ij})^{1/2}}{2\hbar}(t-t_1)\right) + \frac{1}{\xi_{ij}^{1/2}}\sinh\left(\frac{\gamma\xi_{ij}^{1/2}}{2\hbar}(t-t_1)\right)\right] \quad (65)$$

where

$$\xi_{ij} = 1 - \frac{8V_{ij}^2}{\gamma^2} \quad (66)$$

Consequently, we obtain the renormalized second-order memory function as follows

$$M_{ij}(t,t_1) = \frac{2V_{ij}^2}{\hbar^2}\mathrm{e}^{-2\gamma(t-t_1)/\hbar}\left[\cosh\left(\frac{\gamma\xi_{ij}^{1/2}}{2\hbar}(t-t_1)\right) + \frac{1}{(\xi_{ij})^{1/2}}\sinh\left(\frac{\gamma\xi_{ij}^{1/2}}{2\hbar}(t-t_1)\right)\right] \quad (67)$$

Through such treatment, many powers of the second-order correlation function of $V_I(t)$ are incorporated in the above memory function.

6. Numerical Calculations

We make numerical analysis to investigate how much the renormalization effect is significant depending on the magnitude of the coupling strength U and the coherence-destructive force γ in clusters. For such analysis, we define the following normalized memory function

$$C_{ij}(\mu) = \frac{M_{ij}(\mu+t',t')}{M_{ij}(0,0)} \quad (68)$$

6.1. EET in Trimer. We consider a trimer in linear chain. Each molecule is coupled to the neighboring molecule with the same coupling strength $V_{ij}(\equiv U)$. We put the same site energy for the three molecules. We examine in detail the renormalization effect of the memory function in the case that the two-time correlation function is expressed by an exponential form as eq 62, in which case the renormalized memory function is analytically obtained as eq 67. We put $\gamma = 140\ \mathrm{cm}^{-1}$. We consider the three cases of $U = 300$, 140, and 70 cm^{-1}.

The calculated results of the second-order memory function and the renormalized memory function for the three cases of U are plotted in Figure 3. As we see from eqs 66 and 67, $C(\mu)$ oscillates with a period of $4\pi i\hbar/(\gamma\xi^{1/2})$ in the case that U is larger than $2^{1/2}\gamma/4$. Since this critical value is 49 cm^{-1}, all the renormalized memory functions in Figure 3 are oscillatory. When $U = 300\ \mathrm{cm}^{-1}$, $C(\mu)$ is oscillating strongly with a period of 80 fs. As U becomes small, the time profile of $C(\mu)$ approaches to the second-order memory function of the exponential form.

We solve the GME under the condition that the excitation energy is initially located at the first molecule. The calculated results are shown in Figure 4. The red curves are the probability obtained by using the renormalized memory function. The green curves are the probability obtained by using the second-order memory function. The black curves are the probability obtained by solving the PME as follows

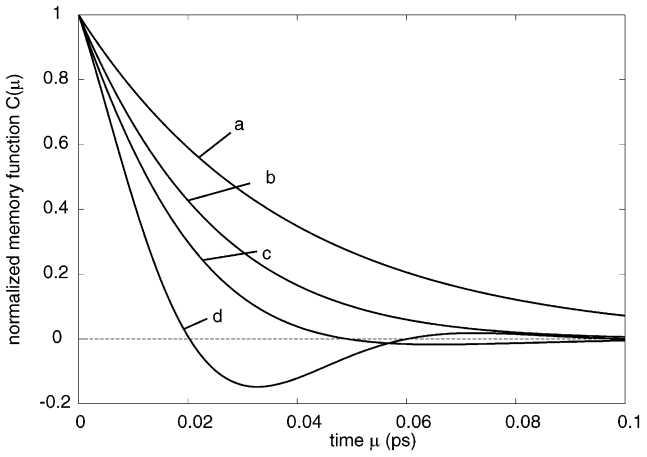

Figure 3. Normalized memory function $C(\mu)$ in the case that the two-time correlation is expressed by an exponential form. (a) Second-order memory function. (b) Renormalized memory function ($U = 70$ cm^{-1}). (c) Renormalized memory function ($U = 140$ cm^{-1}). (d) Renormalized memory function ($U = 300$ cm^{-1}). The coherence-destructive strength γ is 140 cm^{-1}.

$$\frac{dP_i(t)}{dt} = \sum_{k \neq i} \{k_{ik}P_k(t) - k_{ki}P_i(t)\} \tag{69}$$

with

$$k_{ik} = \frac{2U^2}{\hbar\gamma}$$

for neighboring i and k and

$$k_{ik} = 0 \tag{70}$$

for others.

Part A of Figure 4 is the case $U = 300$ cm^{-1} which belongs to the stronger coupling region ($U > \gamma$) within the intermediate coupling regime. We find that the probability $P_1(t)$ of the black curve decreases very sharply, and $P_1(t)$'s of red and green curves decrease moderately. Then, the EET rate calculated by the PME is several times faster than that calculated by the GME with memory functions of the second-order purturbation and the renormalized one. It is seen that $P_1(t)$ obtained using the second-order memory function oscillates largely while $P_1(t)$ obtained using the renormalized memory function oscillates weakly. We also plotted the probability of the excitation energy being located at the third molecule $P_3(t)$. We find that the increase of $P_3(t)$ of the black curve is very rapid and smoothly approaches to the stationary state value. We also find that $P_3(t)$ of the green curve increases slowly and oscillates with large amplitude and that $P_3(t)$ of the red curve oscillates with smaller amplitude. Namely, renormalization works to reduce the oscillatory behavior. The oscillatory behaviors of the green curves of $P_1(t)$ and $P_3(t)$ have a certain phase relation to each other, indicating that the coherent exciton state is almost completely formed throughout the trimer. In the case of red curves, such phase relation is less clearly seen, indicating that the coherent exciton state of trimer is only incompletely formed when the renormalization effect is introduced into the memory function.

Part B of Figure 4 is the case $U = 140$ cm^{-1} which will be almost central ($U \simeq \gamma$) in the intermediate coupling regime. Also in this case, the decrease of $P_1(t)$ of the black curve is very rapid as compared with those of the red and green curves. The green curve shows an oscillatory behavior with considerable

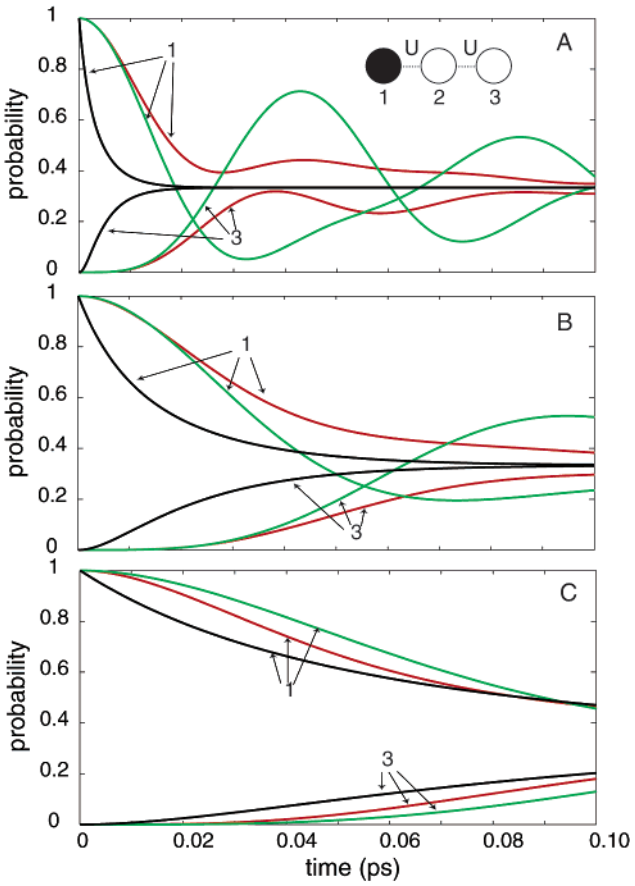

Figure 4. Calculated time courses of the probability that the first or third molecule is excited. At $t = 0$, the first molecule is excited. The black curve is obtained by solving the PME. The green curve is obtained by solving the GME with the second-order memory function. The red curve is obtained by solving the GME with the renormalized second-order memory function. The excitonic coupling strength is (A) 300 cm^{-1}, (B) 140 cm^{-1}, and (C) 70 cm^{-1}, respectively. The number attached to the curve refers to the molecular number.

amplitude. The red curve depresses its oscillatory behavior. The increase of $P_3(t)$ of the black curve is considerably rapid as compared with those of the red and green curves. The $P_3(t)$ of the green curve represents considerable oscillatory behavior while $P_3(t)$ of the red curve does not. This result indicates that the coherent exciton state is formed when the second-order memory function is used and that it is not when the renormalization effect is introduced.

Part C of Figure 4 is the case $U = 70$ cm^{-1} which belongs to the weaker coupling region ($U < \gamma$) within the intermediate coupling regime. The behavior of $P_1(t)$ and $P_3(t)$ of the red, green, and black curves became rather similar although considerable differences remain in the time region 10−80 fs. It is interesting to see that the deviation of $P_1(t)$ of the green curve from that of the red curve exists from very early in time, which was not seen in parts A and B of Figure 4. The red curves oscillate no more and almost monotonically approach to the equilibrium state ($P_1(t) = P_3(t) = 1/3$). No explicit exciton state exists even when the second-order memory function is used.

As summary, the probabilities $P_1(t)$ and $P_3(t)$ calculated by the PME approach the equilibrium state most rapidly without oscillation in all the cases. The probabilities calculated using the second-order memory function are most likely to oscillate, and its amplitude is quite large when U is larger than γ, and the oscillation ceases when U is considerably smaller than γ. The renormalization of the memory function works to decrease

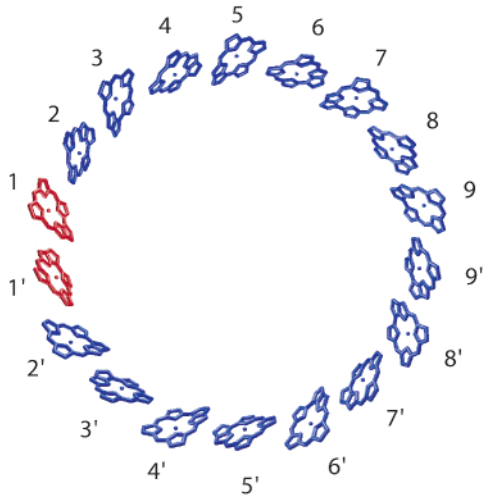

Figure 5. Configulation of the BChla molecules in B850 ring.

the oscillatory behavior of the probabilities calculated using the second-order memory function.

6.2. EET in B850 Ring. Next, we consider the case of EET in the B850 ring,[3] which is a part of the light harvesting antenna system 2 (LH2) in photosynthetic purple bacteria *Rhodopseudomonas (Rps.) acidophila*. Recently, we analyzed the mechanism of EET of the reconstituted B800 → B850 in LH2 and we showed that the GME is useful.[14] From such analysis, we concluded that the EET of B800 → B850 is most suitably expressed as an EET from the locally excited state of B800 to the locally excited states of BChla molecules in B850 which locate nearby the excited BChla molecule in B800.[14] In this study, we clarified the physical reasoning of why the exciton state of B850, which is observed in the optical absorption, cannot be used in the EET of B800 → B850.[14] Under such a situation, it is interesting to see how the excitation energy, which was given to the localized excited state in B850, is delivered to the other members of molecules in B850 by applying the present theory of clusters.

We illustrated B850 ring in Figure 5 and numbered each BChla molecule as 1, 2, ..., 9, 9′, ..., 2′, 1′. In the following numerical calculations, we assume that the excitation energy is initially localized at the two BChla molecules in B850. Namely, we put the initial probability as $P_1(0) = P_{1'}(0) = 0.5$. This is not a dimer exciton state, but the two molecules are excited independently with equal probability. In this calculation, U is put as 300 cm^{-1} for all the neighboring molecules. The site energy of BChla in B850 is put at 12 340 cm^{-1} (810 nm) for all the sites. The absorption spectrum shape $I_i(E)$ of a BChla in the absence of exciton coupling in B850 is taken from the absorption spectrum of BChla in solution.[36] The shape of the fluorescence spectrum $L_j(E)$ of a BChla is substituted by that of Chla in solution except for the position of the peak since no reliable fluorescence spectrum of BChla was obtained.[15] The fluorescence spectrum of Chla and the absorption spectrum of BChla in the B850 are shown in the inset of Figure 6. We find that both spectra have a bump or shoulder which effectively makes the spectral overlap large.

We compare the calculated memory function obtained by the second-order perturbation with that by the renormalization in Figure 6. The dotted curve is the second-order memory function, and the solid curve is the renormalized memory function. Both memory functions initially show a sharp decrease with the time constant of about 5 fs and then a plateau region around 10−25 fs. This initial sharp decrease and the presence of the plateau

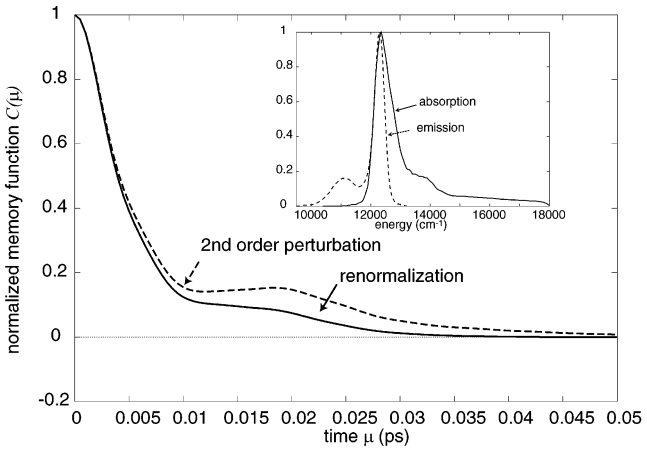

Figure 6. Calculated time courses of the renormalized memory function and second-order memory function using the spectral overlap integral. The inset is the experimental data of the absorption spectrum of Chla, which is a substitution of BChla and the fluorescence spectrum of BChla in solution. The Q_x band is deleted from the fluorescence spectrum.

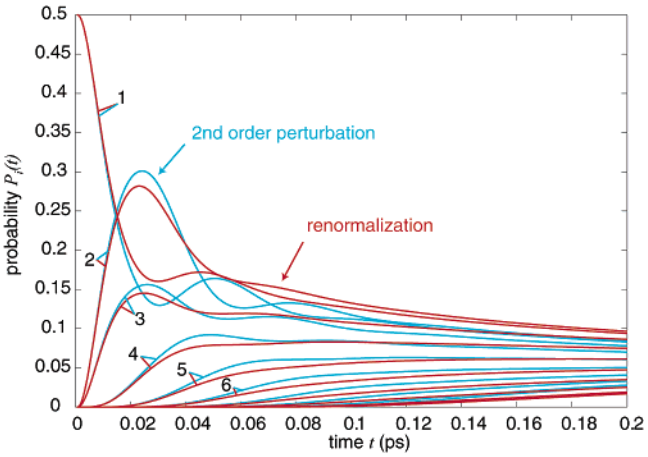

Figure 7. Calculated time courses of the probabilities $P_i(t)$'s of B850. At $t = 0$, 1 and 1′ BChla molecules are excited. The red curve is obtained by solving the GME with the renormalized memory function. The blue curve is obtained by solving the GME with the second-order memory function.

region are present due to the bump or shoulder in the optical absorption and fluorescence spectra.[14] The renormalization effect is to decrease the amplitude of the plateau of the second-order memory function.

In Figure 7, we plot the probabilities calculated by the GME using the second-order memory function (blue curve) and the renormalized memory function (red curve). We find that $P_1(t)$, $P_2(t)$, and $P_3(t)$ of blue and red curves represent remarkable oscillatory behaviors until about 50 fs. The amplitude of the oscillatory part of the blue curve is larger than that of the red curve but its difference is rather small. The probability $P_4(t)$ increases with a much smaller rate than $P_2(t)$ and $P_3(t)$. Probabilities $P_5(t)$ and $P_6(t)$ have no maximum and increase with a much smaller rate than $P_4(t)$. After about 100 fs, all the probabilities monotonically go to converge to the stationary state value of $^1/_{18}$. The converging rates of the red curves are a little smaller than those of the blue curves. The probabilities of $P_{1'}(t)$, ..., $P_{9'}(t)$ are the same as those of $P_1(t)$, ..., $P_9(t)$, respectively. Both are in the relation of mirror image.

In Figure 8, we plot the probabilities calculated by the GME using the renormalized memory function (red curve) and by the PME (green curve). The red curve is the same as Figure 7. The green curves do not show any oscillatory behavior: $P_1(t)$

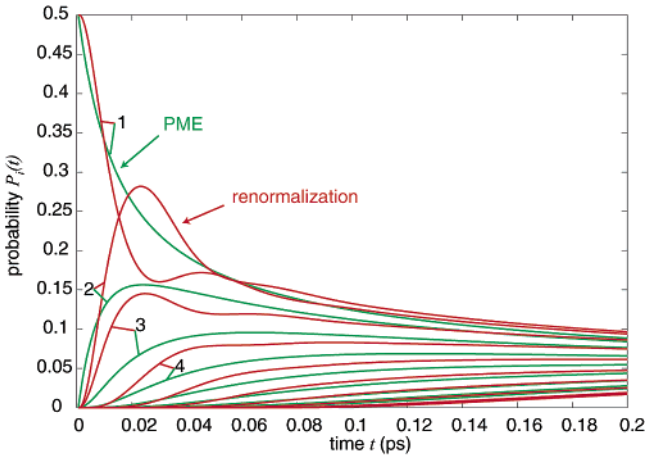

Figure 8. Calculated time courses of the probabilities $P_i(t)$'s of B850. At $t = 0$, 1 and 1′ BChla molecules are excited. The red curve is obtained by solving the GME with the renormalized memory function. The green curve is obtained by solving the PME.

decreases monotonically, $P_2(t)$ increases rapidly and reaches maximum by receiving the excitation energy from the site 1 and decreases monotonically by releasing the excitation energy to the site 3 and so on. All the probabilities begin to increase from time zero but with different rates and turn to converge to the stationary value after about 100 fs. The converging rates of the green curves are a little larger than those of the red curves. These are typical behaviors of EET by the incoherent hopping mechanism involved in the PME.

As a conclusion of the numerical calculations of the EET inside the B850, the probabilities in the early time region calculated by the GME display the formation of coherent character of partly delocalized excitation while those calculated by the PME do not. The renormalization effect to the second-order memory function is to make moderate the oscillatory property of the probabilities in the early time region. The partly delocalized exciton state is delivered to the other molecular sites and the incomplete coherent state extends over the ring at the latter time. Eventually, the difference among the time courses of the probabilities at the latter time calculated by the GME and PME appears to be small.

6.3. Examination of the Usefulness of the Exponential Form for the Second-Order Memory Function. We have derived the analytical form of the renormalized memory function as eq 67 when the second-order memory function is expressed as an exponential form. We examine how much we can obtain a proper solution of GME by replacing the experimentally evaluated second-order memory function by an exponential form. We do it for the EET of B850 in section 6.2. We simulate the second-order memory function by an exponential form as follows

$$M_{ij}(\mu+t',t') = M_{ij}(0,0)\mathrm{e}^{-\gamma\mu/\hbar} \tag{71}$$

where $M_{ij}(0,0) = 2V_{ij}^2/\hbar^2$. We determine the value of γ so that $M_{ij}(\mu+t',t')/M_{ij}(0,0)$ may best fit the experimentally obtained second-order memory function $C(\mu)$ by means of the spectral overlap as follows

$$\gamma = \frac{\hbar}{\int_0^\infty \mathrm{d}\mu C(\mu)} \tag{72}$$

In the case of B850, the experimentally obtained second-order memory function $C(\mu)$ is given as the broken line in Figure 6.

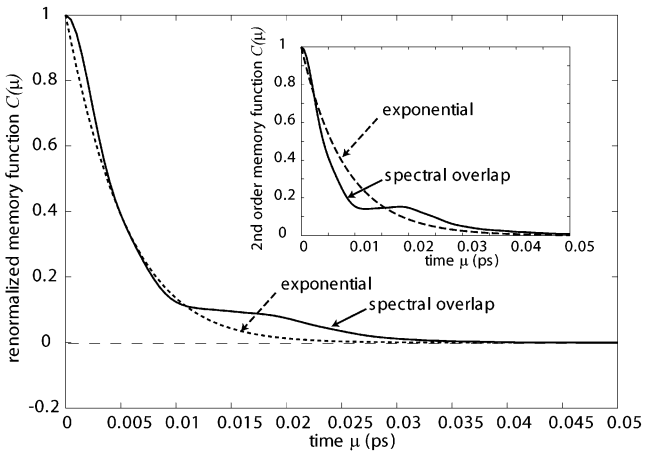

Figure 9. Calculated time courses of the renormalized memory functions obtained from the spectral overlap integral (solid line) and from the second-order memory function best fitted by the exponential form (dashed line). The inset represents the second-order memory functions obtained from the spectral overlap (solid line) and obtained using the simulated exponential function (dashed line). All the memory functions are normalized.

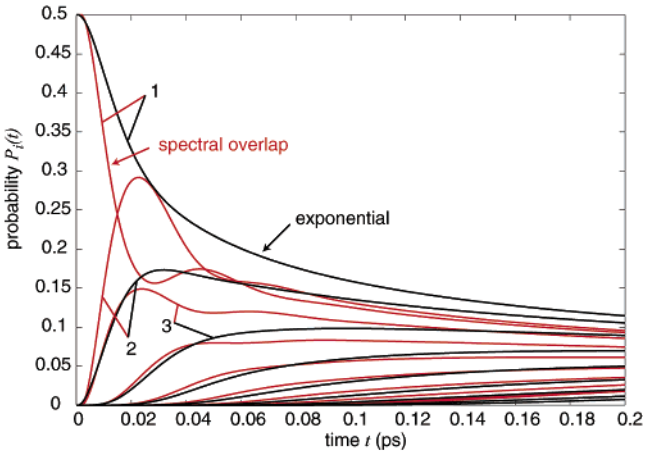

Figure 10. Calculated time courses of the probabilities $P_i(t)$'s of B850. At $t = 0$, 1 and 1′ BChla molecules are excited. The red curve is obtained by solving the GME with the renormalized memory function which is drawn by the solid line in Figure 9. The black curve is obtained by solving the GME with the renormalized memory function which is drawn by the dotted line in Figure 9.

Then, we evaluate $\gamma = 652.6$ cm^{-1} from eq 72. In the inset of Figure 9, we plot the memory function evaluated (on the basis of the present model), indicating the experimental data by a solid curve and the simulated exponential form by a broken curve. In Figure 9, we plot the renormalized memory functions using those second-order memory functions. We find that the dotted curve almost deletes the plateau region of the solid curve. Furthermore, the initial slope of the dotted line becomes much steeper than that of the dotted line in the inset graph; the γ value estimated from the initial slope amounts to about 1000 cm^{-1}.

Then, we solved the GME for the B850 system using the renormalized memory functions in Figure 9. The calculated results are shown in Figure 10. Time profiles of the probabilities obtained by means of the spectral overlap are drawn by red curves which is the same as the red curves in Figures 7 and 8. Time profiles of the probabilities obtained using the simulated exponential form are drawn by black curves. We find that the probabilities of the black curves do not show any oscillatory behavior and so the global feature is similar to the green curves

of PME in Figure 8. The origin of the difference of the black curves from the red curves can be considered as the deletion of the plateau region in the renormalized memory function in Figure 9. This fact indicates that the simulated exponential form for the second-order memory function is not suitable to the EET of B850. More generally, the exponential form for the memory function which is convenient for the theoretical analysis is not necessarily useful for the memory function with plateau region such as that of B850.

7. Discussion

In the previous work, we have constructed a unified theory of the EET for dimers which covers from the weak coupling case to the strong coupling case by self-consistently solving the stochastic Liouville equation with adoption of a certain kind of decoupling procedure.[19] In contrast to this, such a unified theory was not obtained for the cluster until the present time. In the current study using the Redfield theory,[5,22] they approached the intermediate coupling case, using a coherent exciton state as a base and adopting the second-order perturbation of the exciton−phonon interaction. In the Kenkre−Knox theory,[27] they approached the intermediate coupling case using a localized excited state as a base and adopting the second-order perturbation of the excitonic interaction. Therefore, there were no sufficient theories treating the EET in the intermediate coupling case of clusters where $U \sim \gamma$ holds.

Under such situations, in the present paper, we made advancement by the two steps toward the intermediate coupling theory, based on the GME method. One step is an extension of the Kenkre−Knox theory so that the EET from the excited state of the donor during the vibrational relaxation can be treated. Such a process is important in the EET where the EET time is comparable with the vibrational relaxation time. This EET is called the hot transfer, which is one of typical phenomena in the intermediate coupling regime.

The advancement in the second step is the introduction of the renormalization function to the second-order memory function, which is shown in eq 43. Since $R_{ij}(E,t,t_1)$ is obtained by solving the integro-differential eq 61, $R_{ij}(E,t,t_1)$ involves the effect of the powers of combination of the fourth- and second-order time-corrlelation functions. The importance of such a renormalization effect increases as the coupling strength increases as shown in parts A−C of Figure 4.

Detailed numerical calculations are made for the nonamer in the linear chain of B850 in the photosynthetic antenna system. In this system, the coupling strength U is rather large ($\sim$300 cm^{-1}) and the coherence-destructive strength γ is very large (γ is about 650 cm^{-1}, which is obtained when the second-order memory function is simulated by the exponential form in Figure 9). Usually, it was considered that the coherent exciton state will prevail in B850.[5−10] However, we have shown in the present study that the coherent exciton state is not stable (coherent memory time is 20−50 fs as estimated from Figures 6−8). This is because the exciton destructive force is strong. It appears that the coherence-destructive force is strengthened by the presence of the bump or shoulder in the optical absorption and fluorescence spectra.[14]

Oscillatory behaviors of the probabilities of the red and blue curves in Figure 7 represent the coherent property of the EET. To see the detail of the oscillatory parts, $P_2(t)$ and $P_3(t)$ become maximum at time $\sim$25 fs when $P_1(t)$ becomes minimum. Similarly, $P_2(t)$ and $P_3(t)$ have a hollow at time $\sim$50 fs when $P_1(t)$ becomes almost maximum. After 50 fs, no such correlation is found. The above result indicates that time courses of $P_2(t)$ and $P_3(t)$ keep almost an inverse phase relation with time course of $P_1(t)$. The time course of $P_3(t)$ keeps almost the same phase relation as the time course of $P_2(t)$. Such phase relation is most remarkably seen at the first peak of $P_2(t)$ and $P_3(t)$ and almost ceases after about 50 fs. The existence of the above phase relation indicates that the excitations at the sites 1, 2, and 3 are coherently coupled, and so apparently an exciton state with a coherence length of 3 is formed until about 25 fs. This coherent relation among the three sites continues until about 50 fs. This fact will indicate that the localized exciton state of trimer, which, once formed, is not stable as it is but the excitation energies are delivered to the other sites of the ring successively. Even in such a case, the excitonic character of the coherence length of about 3 will be effectively held as a balance of the competitive two forces of the excitonic coupling strength and the coherence-destructive strength in the stationary state.[16] The coherence length of B850 was experimentally evaluated as 2.8 by the experimental observation of superradiance.[37] This value is close to the coherence length obtained by the above calculations. This value is also close to the value estimated from the form of the memory function.[14]

We have seen that the global feature of the black curves in Figure 10, which were obtained by using the exponential form of the second-order memory function, is similar to that of the green curves in Figure 8, which were obtained by the PME method. However, if we compare them in detail, we find some differences. Initial slopes of $P_1(t)$ and $P_2(t)$ of the black curves are rounded while those of the green curves are linearly sharp. A trace of the concave is seen in the $P_2(t)$ of the black curve at about 50 fs while no such structure is seen in the $P_2(t)$ of the green curve. The convergence of all the $P_i(t)$'s of the black curves to stationary values is considerably slower than that of the green curves. These facts suggest that a small amount of excitonic coherency is involved between $P_1(t)$ and $P_2(t)$ of the black curves in the early time and that it is delivered to the other sites in the latter time. Previously, we obtained an empirical formula of the coherence length N_{coh} by using the exponential form of the correlation function as follows[16]

$$N_{\mathrm{coh}} = 1.38 + 1.33\,\frac{U}{\gamma} \tag{73}$$

Substituting $U = 300$ cm^{-1} and $\gamma = 1000$ cm^{-1} as estimated from the dotted line in Figure 9 into eq 73, we obtain $N_{\mathrm{coh}} = 1.78$. This value is consistent with the above result of the black curves in Figure 10 that give the exciton coherence length between 1 and 2.

In the EET in B850, we found that the renormalized memory function has a specific feature of the initial sharp decrease and plateau region at the latter time and it gives a significant effect for the EET mechanism. By fitting the second-order memory function into exponential form, we obtained the renormalized memory function in which the original plateau region is erased. If we solve the GME by using this renormalized memory function, the excitonic coherence property is greatly weakened as shown by the black curves in Figure 10. From these results, we can conclude as follows: Although an exponential form of the memory function is useful for the analysis of the EET mechanism because the analytical treatment is available, the calculated time profiles of the probablities can be drastically different ones when the memory funciton is not simmilar to an exponential form. So far, we defined the coherence-destructive strength γ in the case that the memory function or the correlation function is expressed by an exponential form. Consequently, we need a new-order parameter expressing the coherence-

destructive strength which is applicable to any form of memory function. This work will be done hereafter.

In many photosynthetic antenna systems, BChla or Chla molecules are used as light-harvesting pigments. Therefore, those memory functions should be similar to the one in Figure 6. The excitonic coupling strength U in PS I of *Synechoccus elongatus* was estimated to be in the range of 40∼300 cm^{-1}.[38] This range of the coupling strength will also apply to the other antenna systems. Then, the EET in most of the antenna systems should belong to the weak coupling and/or the intermediate coupling regime. Therefore, the GME method developed in this study will be most suitably applied to the EET of those antenna systems. It is interesting to compare the EET's in the PS I calculated by the GME method with those previously analyzed by the PME method.[38−40] This work is done hereafter.

8. Conclusion

In this paper, we extended our previous theory of the EET in the intermediate coupling case for the dimer to the cluster by using the GME to establish the EET theory, which is applicable to the intermediate coupling case of clusters. In the first, we formulated the second-order memory function from the general point of view. This memory function could be connected to the overlap of the time-dependent fluorescence and absorption spectra of constituting molecules in the cluster system. We showed that the memory function reduces to the Kenkre−Knox formula when we assume that the thermal equilibrium exists in the initial excited state. Our theory also reduces to the Sumi formula of the hot EET when we apply Markovian approximation to the memory function. In the next step, we introduced the renormalization function to the second-order memory function by incoorporating a possible effect due to the powers of combination of the fourth- and second-order time-correlation functions. In numerical calculations of EET in trimer, it was shown that this renormalization effect is quite significant when the coupling strength is larger than the coherence-destructive strength. In the application of the GME method to the EET among BChla molecules inside the B850, we showed that the second-order memory function is much more specific; the memory function initially decays very rapidly with a time constant of about 5 fs and has a plateau in the time range 10−25 fs. Later, it decays slowly. The exciton coherence length calculated by the GME using this specific memory function is about 3 BChla units, which is much smaller than the exciton coherence length observed in the optical absorption of the exciton state.[5] This fact just suggests that the different exciton coherence length is obtained when the observation is made by different means.[14] The above results of relatively small coherence length appear to apply to many of the photosynthetic antenna systems. As shown in this paper, the renormalization effect to the EET in the BChla aggregates is rather small and those EETs belong to the weak coupling or the intermediate coupling regime. We expect that the same thing should happen for the Chla and/or Chlb aggregates, judging from the similar spectral forms of optical absorption and fluorescence to those of BChla. Therefore, we expect that the present GME method, which is applicable to both the weak coupling and intermediate coupling regimes, will be a useful theory for the analysis of the EET mechanism of much more complex systems such as PS I and PS II.

Appendix A. Time-Dependent Probability

In this appendix, we derive eq 9 in accordance with ref 29 and we use the second-order perturbation method with respect to $K_j(t)$ by assuming that $|K_j(t)|$ is sufficiently small. Thus, we first expand the propagator $\exp_+\{-(i/\hbar)\int_0^t \mathscr{H}(t')\,dt'\}$ with respect to $V_1(t')$. Extracting the nonvanishing $P_i(t)$ in the second-order term of $V_1(t')$, we obtain it as follows

$$P_i(t) \equiv \frac{1}{\hbar^2}\int_0^t d\tau \int_{-2(t-\tau)}^{2(t-\tau)} d\sigma \sum_{jj'} \mathrm{Tr}[\rho_p \langle j'|e^{iH\sigma/2\hbar}e^{iH(t-\tau)/\hbar}|i\rangle \times \langle i|e^{-iH(t-\tau)/\hbar}e^{iH\sigma/2\hbar}|j'\rangle e^{-iH_p\sigma/\hbar}]\Xi_{jj'}(\tau,\sigma)e^{-iE\sigma/\hbar} \quad \text{(A1)}$$

where we defined $\Xi_{jj'}(\tau,\sigma) = K_j(\tau + \sigma/2)K_{j'}{}^*(\tau - \sigma/2)$ which is the profile of the incident photon. We approximate $\Xi_{jj'}(\tau,\sigma)$ as $\Xi_{jj'}(\tau,0) \equiv \delta_{jj'}A_j(\tau)/2\pi$, $e^{iH\sigma/2\hbar}$ as $e^{iH_m\sigma/2\hbar}$, and $2(t-\tau)$ in the upper limit of the integration as ∞ since σ is the short time that is necessary for the photoabsorption of the donor. And, because we consider the EET by the light pulse excitation, we approximate the pulse profile by $A_j(\tau) = \hbar P_{0j}\delta(\tau - \epsilon)|_{\epsilon\to+0}$ where P_{0j} is the normalization factor. Then, we obtain the probability $P_i(t)$ at the ith state as follows

$$P_i(t) \equiv \sum_j \frac{P_{0j}}{2\pi\hbar} \times \int_{-\infty}^{\infty} d\sigma e^{-iE\sigma/\hbar}\mathrm{Tr}[e^{iH_j\sigma/2\hbar}e^{-iH_p\sigma/\hbar}\rho_p e^{iH_j\sigma/2\hbar}\langle j|e^{iHt/\hbar}|i\rangle\langle i|e^{-iHt/\hbar}|j\rangle] \quad \text{(A2)}$$

Thus, using the relations of $|d\rangle\langle d| + \sum_i |i\rangle\langle i| = 1$ and $\langle i|e^{iHt/\hbar}|d\rangle = 0$, we get

$$\sum_i P_i(t) = \sum_j \frac{P_{0j}}{2\pi\hbar}\int_{-\infty}^{\infty} d\sigma e^{-iE\sigma/\hbar}\mathrm{Tr}[\rho_p e^{iH_j\sigma/\hbar}e^{-iH_p\sigma/\hbar}] \quad \text{(A3)}$$

This is proportional to the linear combination of the absorption spectrum $I_i(E)$ of each molecule, which was defined as eq 21. Then, in order that the total probability $\sum_i P_i(t)$ preserves 1 for any energy of an initial photon, the normalization factor P_{0j} in the case of $I_j(E) \neq 0$ for all of j can be expressed as $P_{0j} = C_j/I_j(E)$ where $\sum_j C_j = 1$ held. Hence, the probability at the ith site when $t = 0$ is obtained as $P_i(0) \equiv C_i$. Consequently, the probability $P_i(t)$ can be rewritten as follows

$$P_i(t) \equiv \sum_j \frac{P_j(0)}{2\pi\hbar} \times \int_{-\infty}^{\infty} d\sigma \frac{e^{-iE\sigma/\hbar}}{I_j(E)}\mathrm{Tr}[e^{iH_j\sigma/2\hbar}e^{-iH_p\sigma/\hbar}\rho_p e^{iH_j\sigma/2}\hbar\langle j|e^{iHt/\hbar}|i\rangle\langle i|e^{-iHt/\hbar}|j\rangle] \quad \text{(A4)}$$

This is equivalent to eq 9 together with eq 10.

Appendix B. Generalized Master Equation

In this appendix, we derive some important formulas related to the GME by the more general scheme than before. The time-dependent projection operator $X(t)$ defined in eq 46 satisfies the following equations

$$X(t')X(t) = X(t) \quad \text{(B1)}$$

$$Y(t')X(t) = 0 \quad \text{(B2)}$$

$$Y(t')Y(t) = Y(t') \quad \text{(B3)}$$

where we defined the projector $Y(t) = 1 - X(t)$. Then, time derivatives of the projectors satisfy the following relations

$$\dot{X}(t')Y(t) = \dot{X}(t') \tag{B4}$$

$$\dot{Y}(t')Y(t) = \dot{Y}(t') \tag{B5}$$

We consider the following differential equation about any operator $U(t)$

$$\frac{\mathrm{d}U(t)}{\mathrm{d}t} = -\frac{i}{\hbar}W(t)U(t) \tag{B6}$$

where $W(t)$ is any time-dependent operator. Multiplying the projector $X(t)$ to both sides of eq B6 from the left-hand side, and using the relation of eq B4, we obtain the following equation

$$\frac{\mathrm{d}X(t)U(t)}{\mathrm{d}t} = -\frac{i}{\hbar}X(t)W(t)X(t)U(t) - \frac{i}{\hbar}(X(t)W(t) + i\hbar\dot{X}(t))Y(t)U(t) \tag{B7}$$

Similarly we obtain

$$\frac{\mathrm{d}Y(t)U(t)}{\mathrm{d}t} = -\frac{i}{\hbar}Y(t)W(t)X(t)U(t) - \frac{i}{\hbar}(Y(t)W(t) + i\hbar\dot{Y}(t))Y(t)U(t) \tag{B8}$$

We can easily solve eq B8 and then represent $Y(t)U(t)$ as follows

$$Y(t)U(t) = \exp_+\left[-\frac{i}{\hbar}\int_{t_0}^{t}\mathrm{d}t_1(Y(t_1)W(t_1) + i\hbar\dot{Y}(t_1))\right]Y(t_0)U(t_0) - \frac{i}{\hbar}\int_{t_0}^{t}\mathrm{d}t_1\exp_+\left[-\frac{i}{\hbar}\int_{t_1}^{t}\mathrm{d}t_2(Y(t_2)W(t_2) + i\hbar\dot{Y}(t_2))\right]Y(t_1)W(t_1)X(t_1)U(t_1) \tag{B9}$$

Hence, substituting eq B9 into eq B7, we obtain the following closed equation for $X(t)U(t)$

$$\frac{\mathrm{d}X(t)U(t)}{\mathrm{d}t} = -\frac{i}{\hbar}X(t)W(t)X(t)U(t) - \frac{i}{\hbar}(X(t)W(t) + i\hbar\dot{X}(t))\exp_+\left[-\frac{i}{\hbar}\int_{t_0}^{t}\mathrm{d}t_1(Y(t_1)W(t_1) + i\hbar\dot{Y}(t_1))\right]Y(t_0)U(t_0) - \frac{1}{\hbar^2}\int_{t_0}^{t}\mathrm{d}t_1(X(t)W(t) + i\hbar\dot{X}(t))\exp_+\left[-\frac{i}{\hbar}\int_{t_1}^{t}\mathrm{d}t_2(Y(t_2)W(t_2) + i\hbar\dot{Y}(t_2))\right]Y(t_1)W(t_1)X(t_1)U(t_1) \tag{B10}$$

Let us derive the closed equation by use of the Liouville equation under interaction representation of eq 12 and the time-independent projection operator of eq 11. In this case, we put the following corresponce $U(t) = \rho_I(t)$, $W(t) = L_1(t)$, $X(t) = \mathscr{P} = 1 - \mathscr{Q}$, and we can obtain the following equation

$$i\hbar\frac{\mathrm{d}\mathscr{P}\rho_I(t)}{\mathrm{d}t} = \mathscr{P}L_1(t)\mathscr{P}\rho_I(t) + \mathscr{P}L_1(t)\exp_+\left[-\frac{i}{\hbar}\int_0^t\mathrm{d}t_1\mathscr{Q}L_1(t_1)\right]\mathscr{Q}\rho_I(0) - \frac{i}{\hbar}\int_0^t\mathrm{d}t_1\mathscr{P}L_1(t)\exp_+\left[-\frac{i}{\hbar}\int_{t_1}^{t}\mathrm{d}t_2\mathscr{Q}L_1(t_2)\right]\mathscr{Q}L_1(t_1)\mathscr{P}\rho_I(t_1) \tag{B11}$$

Namely, this is the well-known GME.

It should be also pointed out that eq 47 can be derived if we put $W(t) = \mathscr{Q}L_1(t)$ and $U(t) = U(t, t_1)L_1(t_1)$ in eq B10 and use the assumption $Y(t_0)U(t_0,t_1)L_1(t_1) = 0$.

Appendix C. Time-Resolved Fluorescence Spectrum by Pulse Excitation

According to ref 30, the time-resolved fluorescence spectrum of the donor molecule after pulse excitation was defined as follows

$$L(\Omega_1,\Omega_2,t) = \frac{1}{\mathrm{Tr}[A(\Omega_1)]}\int_{-\infty}^{+\infty}\mathrm{d}(\mu/\hbar)\mathrm{Tr}[\mathrm{e}^{i(H_p+\Omega_2)\mu/\hbar}M_2\mathrm{e}^{-iH_j(t+\mu/2)/\hbar}\mathrm{e}^{-\gamma t/\hbar}A(\Omega_1)\mathrm{e}^{-\gamma t/\hbar}\mathrm{e}^{iH_j(t-\mu/2)/\hbar}M_2^{\dagger}] \tag{C1}$$

where

$$A(\Omega_1) \equiv \int_{-\infty}^{+\infty}\mathrm{d}(\sigma/\hbar)\mathrm{e}^{iH_j\sigma/2\hbar}M_1^{\dagger}\rho_p\mathrm{e}^{-i(H_p+\Omega_1)\sigma/\hbar}M_1\mathrm{e}^{iH_j\sigma/2\hbar} \tag{C2}$$

where $M_k^{\dagger}$ is the excitation matrix, $\mathrm{Tr}[A(\Omega_1)]$ is the absorption spectrum, and Ω_1 (Ω_2) is the energy of an incident (emission) photon. We assume that M_k is c number and that $|M_1| = |M_2| \equiv |M|$ under Condon approximation. Then, we rewrite $L(\Omega_1,\Omega_2,t)$ as follows

$$L(\Omega_1,\Omega_2,t) = \frac{|M|^2}{\hbar^2}\int_{-\infty}^{+\infty}\mathrm{d}\mu\langle\mathrm{e}^{iH_j(t-\mu/2)/\hbar-\gamma t/\hbar}\mathrm{e}^{i(H_p+\Omega_2)\mu/\hbar}\mathrm{e}^{-iH_j(\mu/2+t)/\hbar-\gamma t/\hbar}\rangle_{\Omega_1} \tag{C3}$$

where $\langle\cdots\rangle_{\Omega_1} = \mathrm{Tr}[\langle j|\rho_{\Omega_1}|j\rangle\cdots]$. This is proportional to the μ integration of the right-hand side of eq 20, except for the damping term $\mathrm{e}^{-2\gamma t/\hbar}$.

References and Notes

(1) van Grondelle, R.; Dekker, J. P.; Gillbro, T.; Sundstrom, V. *Biochim. Biophys. Acta* **1994**, *1187*, 1.
(2) van Amerongen, H.; Valkunas, L.; van Grondelle, R. *Photosynthetic Excitons*; World Scientific: Singapore, 2000.
(3) McDermott, G.; Prince, S. M.; Freer, A. A.; Hawthornthwalte-Lawless, A. M.; Papiz, M. Z.; Cogdell, R. J.; Isaccs, N. W. *Nature* **1995**, *374*, 514.
(4) Koepke, J.; Hu, X.; Muenke, C.; Schulten, K.; Michel, H. *Structure* **1996**, *4*, 581.
(5) Sundström, V.; Pullerits, T.; van Grondelle, R. *J. Phys. Chem. B* **1999**, *103*, 2327.
(6) Mukai, K.; Abe, S.; Sumi, H. *J. Phys. Chem. B* **1999**, *103*, 6096.
(7) Damjanovic, A.; Ritz, T.; Schulten, K. *Phys. Rev. E* **1999**, *59*, 3293.
(8) Krueger, B. P.; Scholes, G. D.; Fleming, G. R. *J. Phys. Chem. B* **1998**, *102*, 5378.
(9) Leupold, D.; Stiel, H.; Ehlert, J.; Nowak, F.; Teuchner, K.; Voigt, B.; Bandilla, M.; Ücker, B.; Scheer, H. *Chem. Phys. Lett.* **1999**, *301*, 537.
(10) Scholes, G. D.; Fleming, G. R. *J. Phys. Chem.* **2000**, *104*, 1854.
(11) van Oijen, A. M.; Ketelaars, M.; Köhler, J.; Aartsma, T. J.; Schmidt, J. *Science* **1999**, *285*, 400.
(12) Jordan, P.; Fromme, P.; Witt, H. T.; Klukas, O.; Saenger, W.; Krauss, N. *Nature* **2001**, *411*, 909.
(13) Zouni, A.; Witt, H. T.; Kern, J.; Fromme, P.; Krauss, N.; Saenger, W.; Orth, P. *Nature* **2001**, *409*, 739.
(14) Kimura, A.; Kakitani, T. *J. Phys. Chem. B* **2003**, *107*, 7932.
(15) Herek, J. L.; Fraser, N. J.; Pullerits, T.; Martinsson, P.; Polivka, T.; Scheer, H.; Cogdell, R. J.; Sundström, V. *Biophys. J.* **2000**, *78*, 2590.
(16) Kakitani, T.; Kimura, A. *J. Phys. Chem. A* **2002**, *106*, 2173.
(17) Förster, Th. *Ann. Phys.* **1948**, *2*, 55.
(18) Frenkel, J. *Phys. Z. Sowjetunion* **1936**, *9*, 158.
(19) Kimura, A.; Kakitani, T.; Yamato, T. *J. Phys. Chem. B* **2000**, *104*, 9276.
(20) Kühn, O.; Sundström, V. *J. Chem. Phys.* **1997**, *107*, 4154.
(21) Dahlbom, M.; Pullerits, T.; Mukamel, S.; Sundström, V. *J. Phys. Chem. B* **2001**, *105*, 5515.
(22) Redfield, A. G. *Adv. Magn. Reson.* **1965**, *1*, 1.

(23) Kakitani, T.; Kimura, A.; Sumi, H. *J. Phys. Chem. B* **1999**, *103*, 3720.
(24) Kimura, A.; Kakitani, T.; Yamato, T. *J. Lumin.* **2000**, *87*−*89*, 815.
(25) Kakitani, T.; Kawatsu T., Kimura, A.; Yamada, A.; Yamato, T.; Yamamoto, S. *J. Bio. Phys.* **2002**, *28*, 367.
(26) Kimura, A.; Kakitani, T.; Yamato, T. *J. Mod. Phys. B* **2001**, *15*, 3833.
(27) Kenkre, V. M.; Knox, R. S. *Phys. Rev.* **1974**, *B9*, 5279.
(28) Kenkre, V. M. *Exciton Dynamics in Molecular Crystals and Aggregates*, *Springer Tracts in Modern Physics 94*; Springer-Verlag: New York, 1982.
(29) Sumi, H. *J. Phys. Soc. Jpn.* **1982**, *51*, 1745.
(30) Toyozawa, Y. *J. Phys. Soc. Jpn.* **1976**, *41*, 400.
(31) Kubo, R.; Toda, M.; Hashitsume, N. *Statistical Physics II*; Springer: Berlin, 1985; Chapter 5.
(32) Kimura, A.; Kakitani, T., in preparation.
(33) Grabert, H. *Projection Operator Techniques in Nonequilibrium Statistical Mechanics*, *Springer Tracts in Modern Physics 95*; Springer-Verlag: New York, 1982.
(34) Kimura, A.; Kakitani, T., to be published.
(35) Scholes, G. D.; Fleming, G. R. *J. Phys. Chem. B* **2000**, *104*, 1854.
(36) Eichwurzel, I.; Stiel, H.; Teuchner, K.; Leupold, D.; Scheer, H.; Salomon, Y.; Scherz, A. *Photochem. Photobiol.* **2000**, *72*, 204.
(37) Monshouwer, R.; Abrahamsson, M.; van Mourik, F.; van Grondelle, R. *J. Phys. Chem. B* **1997**, *101*, 7241.
(38) Damjanovic, A. A.; Vaswani, H. M.; Fromme, P.; Fleming, G. R. *J. Phys. Chem. B* **2002**, *106*, 10251.
(39) Sener, M. K.; Lu, D.; Ritz, T.; Park, S.; Fromme, P.; Schulten, K. *J. Phys. Chem. B* **2002**, *106*, 7948.
(40) Byrdin, M.; Jordan, P.; Krauss, N.; Fromme P.; Stehlik, D.; Scholdder, E. *Biophys. J.* **2002**, *83*, 433.